Numerical analysis to study the effect of through thickness reinforcement with different stitch orientations on open-hole laminates

P. Joshi*[1], A. Kondo[2] and N. Watanabe[1]

The effect of through thickness reinforced open-hole laminates was analysed in terms of laminate behaviour under in-plane tensile loading based on continuum mechanics. Stitches around the notch were oriented in the longitudinal and transverse directions. To obtain the macroscopic damage and the local stress–strain constitutive behaviour, laminates were modelled on a lamina-wise basis. Interfaces between lamina and stitch yarns were assumed to be perfectly glued and modelled by the contact capability. Discretisation procedures using the principle of virtual work were applied in addition to discretisation of the contact traction. Progressive failure analysis with Puck's failure criteria was conducted to characterise the failure behaviour of the laminate. In both cases, damage was initiated by a matrix crack in the perpendicular direction of the loading axis on the notch. The longitudinally stitched laminate showed a 14.29% higher strength compared to the transversely stitched laminate by suppressing damage propagation. The results obtained using this finite element technique was consistent with the experimental results.

Keywords: Damage, Open-hole tension, Progressive failure, Stress concentration factor, Stress–strain

Introduction

Lightweight composite structures with high strength have been increasingly prevalent in flight vehicles and automobiles which make a significant economic and environmental contribution. Notches and cut-outs on structures are inevitable due to various design requirements. However, discontinuities in the structure are susceptible to damage initiation.[1,2] Through thickness reinforcement (TTR) could be used to strengthen the structural properties. Dransfield *et al.*[3] and Mai and co-workers[4,5] demonstrated that stitching offers considerable promise as a low-cost method for TTR to strengthen in-plane mechanical properties. Mouritz and Cox[6] reported that TTR is not strongly influenced by the volume content or diameter of the reinforced stitch or 3D weaving tows. However, Mouritz's review on GFRP[7] and FRP[8] (limited to woven, knitted and braided composites) noted that there are contradictory reports on whether in-plane properties improve or degrade upon stitching. Findings that report degradation[9,10] of mechanical properties of stitching tend to correlate the reduction with the fibre waviness or misalignment (in-plane and out-of-plane) and breakage of the in-plane fibre and resin rich regions. In contrast, reports that describe an improvement[3–6,11,12] of the in-plane mechanical properties postulate that this improvement is a result of effective suppression of delamination and an increase of the local fibre volume fraction because of the compaction effect. It has been reported that stitching improves or degrades the tensile strength by up to 15–20% compared to unstitched laminates.[4,6,8,9,11–14] Thus, understanding the effect of stitching on composite laminates is essential for the further development of such structures.

Woven fabric has gained attraction because of its lower manufacturing cost and stability at 0° and 90° to unidirectional laminates; it has a complex pattern due to its weft and waft tow interlaces.[15] Different numerical formulation, specific programming, and commercial finite element tools have been employed to solve microstructural problems. Ishikawa and Chou[16,17] proposed a mosaic model, fibre undulation and a bridging 1D model for the study of the thermoelastic behaviour of woven composites. The mosaic model was idealised as an assemblage of asymmetrical cross-ply laminates. Drawbacks of fibre undulation and fibre continuity in the mosaic model were addressed by the undulation model. The bridging model analysed a satin weave woven composite. Naik and Kuchibhotla[18] further developed the 2D model as an extended undulation model. Cox *et al.*[19–21] formulated a binary model using two-node line elements and 8-node solid elements representing axial and transverse tows, respectively. Camanho[22] states that the domain superposition technique by

[1]Department of Aerospace Engineering, Tokyo Metropolitan University, 6-6 Asahigaoka, Hino-shi, Tokyo 191-0065, Japan
[2]e-Xstream Engineering, MSC Software Company, 1-23-7 Nishishinjuku, Shinjuku-ku, Tokyo 160-0023, Japan

*Corresponding author, email joshi-prabij@ed.tmu.ac.jp; aeromecha03@gmail.com

Published by Taylor & Francis on behalf of the Institute
Received 24 June 2016; accepted 30 September 2016
DOI 10.1080/14658011.2016.1245011

independently meshing tows using solid elements. Green *et al.*[15] modelled a 3D satin woven composite unit cell using the TexGen pre-processor following the voxel method and continuum damage model, which was hypothesised to represent the architecture more realistically. However, it has been considered impractical to model interpenetration at tow crossovers at the macroscopic structural level. Focusing on this difficulty, Tong *et al.*[12] identified five different modelling strategies.

At an early stage, Whitney and Nuismer formulated failure criteria for open-hole composite laminates.[23] Since then, numerous experimental and numerical investigations have been carried out for characterisation and prediction of the notch strength of open-hole laminates.[24–28] Despite extensive studies on open-hole laminates, studies on the effect of the stitch on open-hole stitched laminates are limited. Thuis and Bron[29] studied notched strength for different stitching densities and found a reduction of 54% tensile strength at a density of 10 cm^{-2}. Khan and Mouritz[30] and Junqian and Yuqing[31] investigated Kevlar-stitched laminates and reported that stitch orientation does not affect tensile strength. Han *et al.*[32] carried out an experimental investigation on non-woven composite laminates with circular single and double stitching reinforcement around the central hole. Gliesche[33] performed an optical investigation on the open-holed tailored fibre placement process (TFP), implemented to reinforce non-woven composite laminates with a grating method from GOM Corp, and Yudhanto *et al.*[34] experimentally investigated longitudinal and transverse parallel stitched open-hole plain weave woven laminates. These studies agreed with the conclusion that tensile strength is improved by reinforcement.

Research on stitched laminates indicates that strength, stiffness and crack propagation depend upon ply thickness, laminate streaking sequence, stitching thread properties, stitch row spacing, stitch pitch and stitch density.[9,35] Researchers have noted that research on open-hole laminates is concentrated on notch sensitivity depending on the ply thickness, the hole-size and the geometry of the laminate streaking sequence.[24–28] Thus, a detailed study on the effect of stitch orientation or location on discontinuous composite structures to predict damage initiation and progression is expected to add value for designers seeking to enhance the quality of the structure.

This paper presents an evaluation of open-hole carbon-fibre/epoxy (T300/EP3631) stitched laminates in terms of tensile loading at the macroscopic structural level, using Kevlar-29 stitch thread oriented in the longitudinal and transverse directions along the discontinuity. For this study, a simplified macroscopic model has been developed, the lamina and stitching have been discretised based on continuum mechanics, and the interface between them is modelled with contact capability. Second, progressive failure analyses have been performed to characterise the failure behaviour of the laminates. Third, these numerical analyses have been performed to validate the results and determine the in-plane characteristics of the open-hole stitched laminates. Fourth, a comparison has been made between the analytical and numerical solutions for the open-hole stitched laminate stress concentration distribution. Thus, it is capable of capturing the effect of stitching in the vicinity of the discontinuity for damage characterisation, stress–strain behaviour and stress concentration behaviour, which was unclear from the experimental analysis.

Specimen and test details

A coupon test was prepared following ASTM D5766 standard instructions.[36] Specimens measuring 250 mm × 25 mm × 4 mm of T300-3K carbon-fibre/epoxy manufactured by Toray Industries were prepared in which stitches were oriented longitudinally and transversely along the central opening through a hole of 6.35 mm. Stitching was employed with spacing(s) of 12 mm and a pitch (p) of 3 mm by modified locked stitching with 1500 denier Kevlar-29 thread as shown in Fig. 1. The test laminate consists of 20 ply layers, i.e. $[(0/90)_{20}]$. An Instron 8802 tool with a maximum load capacity of 100 kN was used for tensile loading at a rate of 1 mm min^{-1}. Single element strain gauges of type KFG-5-120-C1-23L3M2R with a 5 mm gauge length and 2.10 + 1.0% gauge factor at operating conditions of 24°C and 50% RH were positioned on the laminate surface in quarter bridge configurations.

Macroscale modelling for structural analysis

3D structural modelling and finite element analysis have been carried out for stitched laminates because of their capability to achieve realistic physical representation and in-plane and out-of-plane laminate behaviour analysis. A detail modelling approach with stitching has been incorporated because the idealised model has been reported to overestimate the strength.[26,37] Puck's failure theory has been incorporated into the failure analysis.

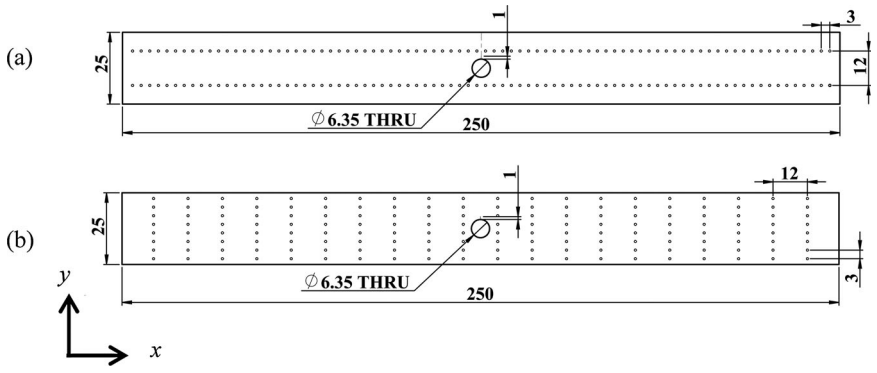

1 Schematic of open-hole laminates: *a* longitudinally stitched; *b* transversely stitched

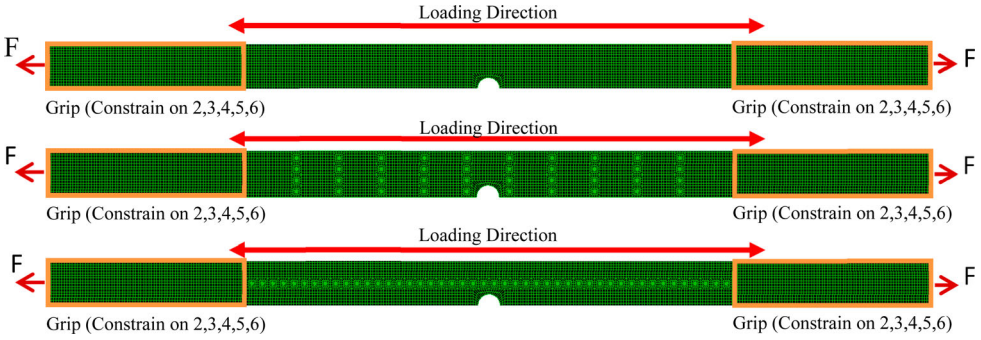

2 Loading and boundary conditions for open-hole laminates

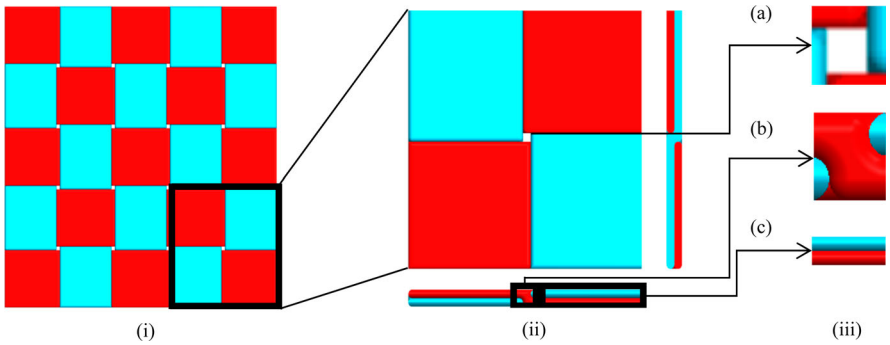

3 Schematic of plain weave woven composite laminates: (i) warp and weft tows arrangement; (ii) cross-section of unit cell; (iii) microstructures of unit cell. *a* Void/pure resin; *b* undulated; *c* straight cross ply

The finite element model of unstitched, transversely and longitudinally stitched open-hole laminates with pertinent boundary condition with a fine mesh after convergence is shown in Fig. 2.

During macroscopic modelling, it is impractical to model microscopic details as shown in Fig. 3 using unit cell modelling. However, a single micro-block configuration can be used as an assembling unit for different types of macro-block patterns and the macro-block to represent the laminate structure.[38] A macro-block, which represents the majority of the structure, is used to represent woven characteristics. Thus, a single solid through thickness element has been adopted that represents the warp and weft yarn. These elements have been so arranged at 0° and 90° so that the internal orientation will represent the combined overall effect of the lamina.

The commercial MSC Nastran/Patran user interface can be used to define the stacking sequence of all lamina of the laminate in a single element with the relevant material properties. During this analysis, a single element per lamina has been employed, in contrast to defining a laminate stacking sequence in a single element through the thickness. In this formulation, lamina properties have been assigned separately in a layer-by-layer manner. The multi-layered material definition for each lamina is shown in Tables 1 and 2. This approach transfers the laminate definition based on the material properties to the lamina geometric orientation defined by the stacking sequence. Nodes between the lamina are shared. This modelling is limited to plain weave woven composites.

Additionally, certain assumptions have been made to cope with the complexity of architecture:

- The plain weave woven fabrics are assumed to be balanced; i.e. the woven fabric unit cell, fibre volume fraction and mechanical properties along the warp direction are identical to those in the weft direction.
- The warp and weft tows are packed perfectly, and the void of resin and nesting resin on the interlacing areas between warp and weft tows are ignored.
- The macro-structure of woven fabric is orthotropic and homogeneous.
- All lamina undergo the same deformation.

For the modelling of stitches, emphasis has been placed on properly characterising the stitching process. The stitching process consists of inserting a needle and carrying a stitch thread through a stack of fabric layers. Fibres

Table 1 Material properties of T800SC-24kf/Epoxy XNR

Fibre tensile strength/GPa	5.49
Fibre compressive strength/GPa	2.6
Matrix tensile strength/MPa	0.8
Matrix compressive strength/MPa	0.5

Table 2 Material properties

	Kevlar-29	T300-3k
Volume fraction/%	…	59
Longitudinal modulus, E_x/GPa	70.5	139.18
Transverse modulus, E_y/GPa	2.59	9.71
Out-of-plane modulus, E_z/GPa	2.59	9.71
In-plane shear modulus, G_{xy}/GPa	2.17	5.58
Out-of-plane shear modulus, G_{xz}/GPa	2.17	5.58
Out-of-plane shear modulus, G_{yz}/GPa	2.17	3.76
Poisson's ratio, ϑ_{xy}	0.36	0.29
Poisson's ratio, ϑ_{xz}	0.0132	0.02
Poisson's ratio, ϑ_{yz}	0.36	0.40

are arranged along two axial lines, and a series of stitch yarn with predefined pitch are thrust into fibre layers.[39] Henceforth, stitching and laminates are discretised in the model. Stitches are represented by a homogeneous solid element. Interfaces between matrix and stitch yarns are assumed to be perfectly glued and are modelled by the type of contact capability used for delamination propagation studies.[40,41] The node-to-surface algorithm of contact detection is adopted to represent contact on the deformable body. Contact is assumed to occur when the element surface penetrates one of the target segment elements on the specified target surface.

Continuum mechanics at lamina

On the lamina level, the fibre-matrix composite is regarded as a homogeneous but anisotropic material. The direction parallel to the fibre is denoted as ∥, and the direction perpendicular to the fibre is denoted as ⊥. On the lamina level, the stress analysis assigns a state of stress to any state of strain or vice versa. The constitutive behaviour, which relates states of stress to states of strain, is then defined by the compliance matrix given as follows:

$$\begin{bmatrix} \varepsilon_1 \\ \varepsilon_2 \\ \varepsilon_3 \\ \gamma_{12} \\ \gamma_{13} \\ \gamma_{23} \end{bmatrix} = \begin{bmatrix} 1/E_{\parallel} & -v_{\parallel\perp}/E_{\perp} & -v_{\parallel\perp}/E_{\perp} & 0 & 0 & 0 \\ -v_{\parallel\perp}/E_{\parallel} & 1/E_{\perp} & -v_{\perp\perp}/E_{\perp} & 0 & 0 & 0 \\ -v_{\parallel\perp}/E_{\parallel} & -v_{\perp\perp}/E_{\perp} & 1/E_{\perp} & 0 & 0 & 0 \\ 0 & 0 & 0 & 1/G_{\parallel\perp} & 0 & 0 \\ 0 & 0 & 0 & 0 & 1/G_{\parallel\perp} & 0 \\ 0 & 0 & 0 & 0 & 0 & 1/G_{\parallel\perp} \end{bmatrix} = \begin{bmatrix} \sigma_1 \\ \sigma_2 \\ \sigma_3 \\ \tau_{12} \\ \tau_{13} \\ \tau_{23} \end{bmatrix} \quad (1)$$

Continuum mechanics formulation for contact

For the analysis of solids and structures with large displacement and large strain, a Lagrangian formulation usually represents a more natural and effective analysis approach. The FE solution of the governing continuum mechanics equation is obtained by using discretisation procedures for the principle of virtual work in addition to contact traction through externally applied forces, and the constraint equation is defined as[42] shown below:

$$\sum_{L=1}^{N} \int_{^{t+\Delta t}V} {}^{t+\Delta t}\tau_{ij}\, \delta_{t+\Delta t} e_{ij}\, d^{t+\Delta t}V = {}^{t+\Delta t}R = \sum_{L=1}^{N} \begin{pmatrix} \int_{^{t+\Delta t}V} \delta u_i\, {}^{t+\Delta t}f_i^B\, d^{t+\Delta t}V \\ + \int_{^{t+\Delta t}S_f} \delta u_i^{S}\, {}^{t+\Delta t}f_i^S\, d^{t+\Delta t}S \end{pmatrix} + \sum_{L=1}^{N} \int_{^{t+\Delta t}S_c} \delta u_i^{c}\, {}^{t+\Delta t}f_i^c\, d^{t+\Delta t}S \quad (2)$$

where ${}^{t+\Delta t}\tau_{ij}$ is the Cartesian component of the Cauchy stress tensor; $\delta_{t+\Delta t}e_{ij} = \frac{1}{2}\left(\frac{\partial \delta u_i}{\partial {}^{t+\Delta t}x_j} + \frac{\partial \delta u_j}{\partial {}^{t+\Delta t}x_i}\right)$ is the strain tensor corresponding to virtual displacement; δu_i is the virtual displacement vector imposed at $t+\Delta t$, a function of ${}^{t+\Delta t}x_j$; ${}^{t+\Delta t}x_j$ is the Cartesian coordinates of material point at $t+\Delta t$; ${}^{t+\Delta t}V$ is the volume at time $t+\Delta t$.

The component of contact tractions is denoted as ${}^{t+\Delta t}f_i^c$ and act over the area ${}^{t+\Delta t}S_c$, and the components of externally applied tractions are denoted as ${}^{t+\Delta t}f_i^S$ and act over the area ${}^{t+\Delta t}S_f$. We assume that ${}^{t+\Delta t}S_f$ is a part of ${}^{t+\Delta t}S_c$ although such an assumption is not necessary.

We consider two bodies *I* and *J* as shown in Fig. 4, with each body supported such that without contact, no rigid body motion is possible.

The virtual work due to contact traction from equation (2) is as follows:

$$\int_{S^{IJ}} \delta u_i^I f^{IJ}\, dS^{IJ} + \int_{S^{JI}} \delta u_i^J f^{JI}\, dS^{JI} = \int_{S^{IJ}} \delta u_i^J f^{IJ}\, dS^{IJ} \quad (3)$$

Let ${}^t f_i^{IJ}$ be a vector of contact surface traction on the body I due to contact with body *J*; then, ${}^t f_i^{IJ} = -{}^t f_i^{IJ}$. Additionally, δu_i^I and δu_i^J are the components of the virtual displacement on the contact surface of body *I* and *J*, respectively. S^{IJ} and S^{JI} are contact pair, not necessarily of equal size.

We can decompose the corresponding contact traction ${}^t f_i^{IJ}$ acting on S^{IJ} into normal and tangent components *n* and *s* on S^{JI} as follows:

$${}^t f^{IJ} = \lambda n + ts \quad (4)$$

where λ and *t* are the normal and tangent traction components. Thus,

$$\lambda = ({}^t f^{IJ})^T n;\; t = ({}^t f^{IJ})^T s \quad (5)$$

To define the actual value of *n*,*s* that can be used in our contact calculation, consider a generic point *x* on S^{IJ}, and let $y^*(x,t)$ be the point on S^{JI} satisfying

$$\|x - y*(x,\, t)\|_2 = \min_{y \in s^{JI}} \{\|x - y\|_2\} \quad (6)$$

The (signed) distance from *x* to S^{IJ} is then given by the gap function *g*:

$$g(x.t) = (x - y*)^T n* \quad (7)$$

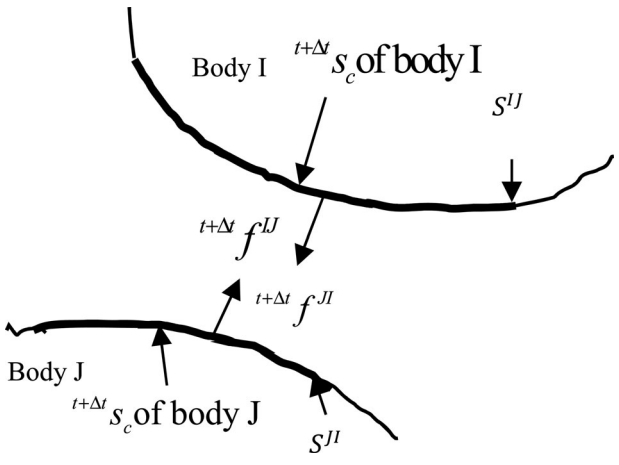

4 Bodies in contact

where n^* corresponding to point x is the unit normal vector at $y^*(x,t)$. Thus, the condition of normal contact definition is as follows:

$$g \geq 0;\ \lambda \geq 0;\ g\lambda = 0 \tag{8}$$

If $g > 0$, then we must have $\lambda = 0$, and vice versa.

Failure criteria

Puck's theory[43] has been the most promising approach for 3D application. The maturity of this failure criterion for the prediction of lamina failures and post-failure analysis has been illustrated on WWFE-II.[44–46] It defines two types of failure: the fibre failure $f_{E,FF}$ and inter-fibre failure (matrix cracking) $f_{E,IFF}$.

The following expression defines fibre failure[43–46]:

$$f_{E,FF} = \frac{1}{\pm R_{\parallel}^{t,c}}\underbrace{\left[\sigma_1 - \left(\nu_{\perp\parallel} - \nu_{\perp\parallel f}\frac{E_{\parallel}}{E_{\parallel f}}\right)(\sigma_2+\sigma_3)\right]}_{a} \tag{9}$$

$R_{\parallel}^{t}$ for a ≥ 0

$-R_{\parallel}^{t}$ for a ≥ 0

The following expression defines inter-fibre failure or matrix failure[43–46]:

$$f_{E,IFF}(\theta) = \sqrt{\left[\left(\frac{1}{R_{\perp}^{t}} - \frac{P_{\perp\psi}^{t}}{R_{\perp\psi}^{A}}\right).\sigma_n(\theta)\right]^2 + \left(\frac{\tau_{nt}(\theta)}{R_{\perp\perp}^{A}}\right)^2 + \left(\frac{\tau_{n1}(\theta)}{R_{\perp\parallel}^{A}}\right)^2} + \frac{P_{\perp\psi}^{t}}{R_{\perp\psi}^{A}}\sigma_n(\theta)$$

for $\sigma_n \geq 0$

$$f_{E,IFF}(\theta) = \sqrt{\left(\frac{\tau_{nt}(\theta)}{R_{\perp\perp}^{A}}\right)^2 + \left(\frac{\tau_{n1}(\theta)}{R_{\perp\parallel}^{A}}\right)^2 + \left(\frac{P_{\perp\psi}^{c}}{R_{\perp\psi}^{A}}\sigma_n(\theta)\right)^2} + \frac{P_{\perp\psi}^{c}}{R_{\perp\psi}^{A}}\sigma_n(\theta)$$

for $\sigma_n < 0$ (10)

Stress concentration factor (SCF)

The SCF for uniaxial in-plane loading in x direction for a balanced symmetric orthotropic infinitely wide laminate

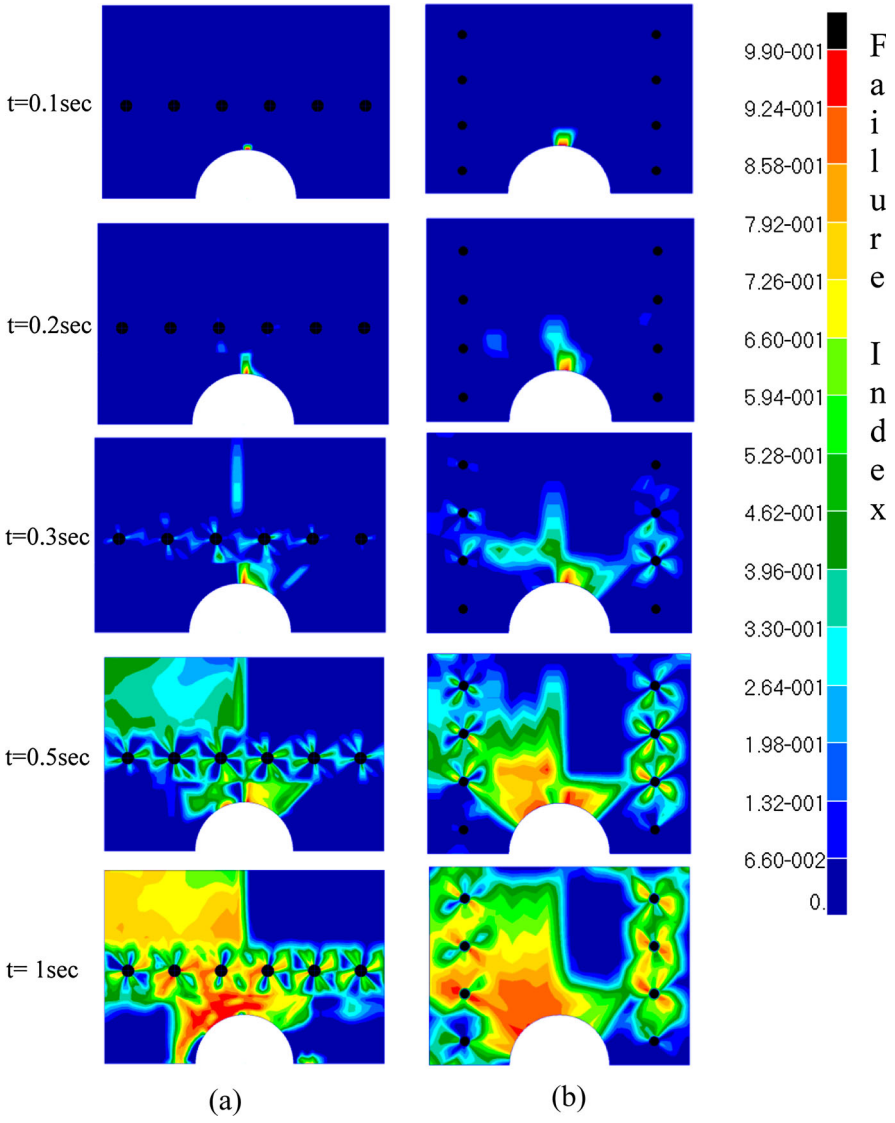

5 Progressive damage analysis of stitched open-hole laminates: *a* longitudinal stitch; *b* transverse stitch

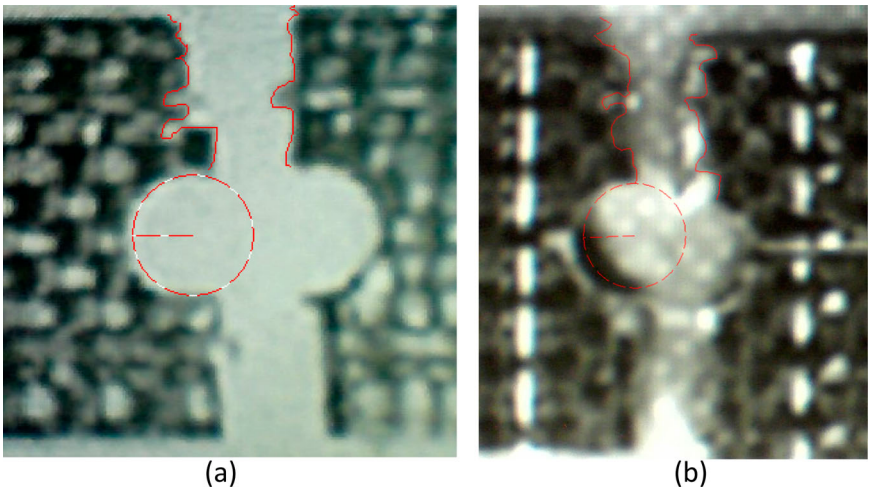

6 X-ray radiography final damage: *a* longitudinal damage; *b* transverse damage

is defined as follows[47]:

$$k_t^{\infty} = 1 + \sqrt{2\left(\sqrt{\frac{E_x}{E_y}} - \nu_{xy} + \frac{E_x}{2G_{xy}}\right)} \tag{11}$$

The theoretical SCF is defined by the maximum stress $\sigma_{\max}$at a discontinuity to nominal stress σ_n computed assuming that the discontinuity is not present; i.e.

$$k_t = \sigma_{\max}/\sigma_n \tag{12}$$

Additionally, the effective SCF $k_e$is given by the following expression[23,47,48]:

$$k_e = \frac{\sigma_x}{\sigma_n} \approx \left[1 + \frac{\xi^2}{2} + \frac{3\xi^4}{2} - \frac{(k_t^{\infty} - 3)}{2}(5\xi^6 - 7\xi^8)\right] f_w \tag{13}$$

where $\xi = (a/y)$, $f_w = 2 + (1 - {}^{2a}/_{w})^3/3(1 - {}^{2a}/_{w})$; a is the radius of the hole; y is the distance from the centre of the hole; f_w is the correction factor for a finite width plate; w is the width of the finite plate.

It has been noted that the correction factor differs by less than 10% from the exact solution in most cases if ${}^{2a}/_{w} \leq {}^{1}/_{3}$.[47]

Normally, k_e is lower than k_t because of a reduced sensitivity of the material to notches. The notch sensitivity is defined as follows:

$$q = \frac{k_e - 1}{k_t - 1} \tag{14}$$

The notch sensitivity ranges from 0 to 1, corresponding to minimal to full sensitivity to the notch.

Stress concentration calculation from the strain

When the mechanical properties of woven fabric laminates are assumed to be orthotropic, the axial stresses around the notch can be calculated from the measured strain from the stress–strain relation using the following expression:

$$\sigma_x = \frac{E_x \varepsilon_x}{1 - \nu_{xy}^2({}^{E_y}/_{E_x})} + \frac{\nu_{xy} E_y \varepsilon_y}{1 - \nu_{xy}^2({}^{E_y}/_{E_x})} \tag{15}$$

Results and discussions

Progressive failure analysis

The progressive damage analysis depicted in Fig. 5*a* and *b* shows longitudinally and transversely stitched open-hole laminates. From Puck's failure criteria, it was found that failure occurred due to matrix failure. Figure 6 depicts

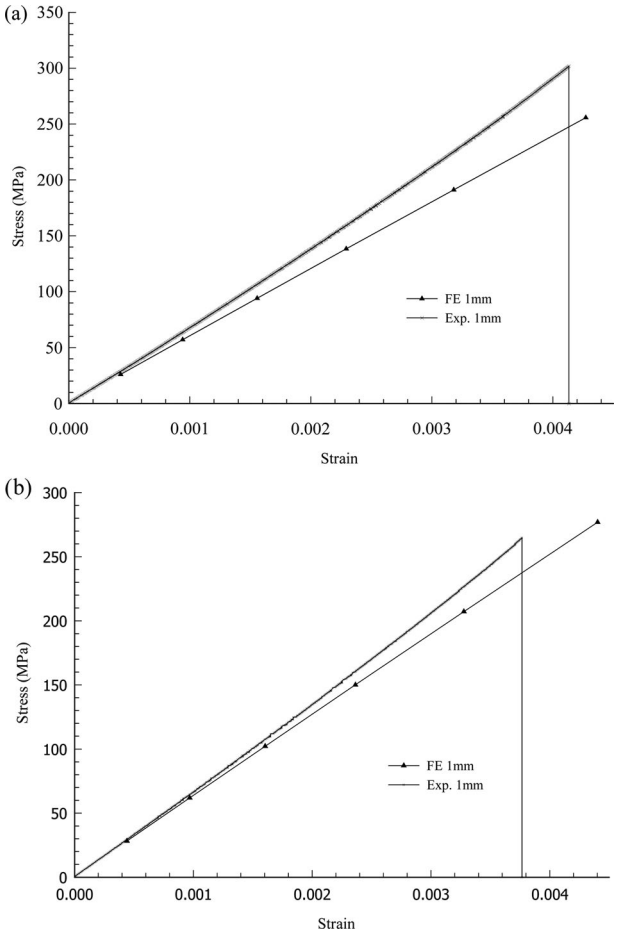

7 Stress–strain distributions of open-hole laminates with different stitch orientation: *a* longitudinally stitched; *b* transversely stitched

the X-ray radiograph of the damaged laminates after the experiment. The FEM result shows that initiation of matrix damage occurred in the direction perpendicular to load application, as shown in Fig. 5 at $t = 0.1$. With the increase in load, this damage propagates towards the characteristic length. At $t = 0.3$, it can be observed that the longitudinal stitch suppresses crack propagation and is capable of withstanding more stress, while at the transverse stitch, crack propagation occurs.

In the layer-wise failure analysis defined by Puck, a macroscopic crack through an entire lamina causes failure of the lamina. The damaged portion of the lamina no longer transmits any load, but neighbouring laminae still apply load onto the undamaged sections of the damaged lamina. This load transmission results in the multiplication of cracks if more load is applied. At $t = 0.3$, it can be observed that damage was initiated at the contact region between the stitch and laminates, which signifies matrix debonding of the stitch at the resin-rich region. This debonding eventually leads to fibre breakage. This phenomenon has also been observed in 2D orthogonal stitched laminates.[49] Thus, a simultaneous matrix-crack followed by fibre-matrix debonding finally leads to catastrophic failure of the laminate. In both cases, FEM analysis is able to predict damage effectively, as correlated by the X-ray radiography shown in Fig. 6.

From Figs. 5 and 6, it can be concluded that the laminates are affected by the stitch orientations. It can also be observed that the longitudinally stitched laminate (LSL) is more effective than the transversely stitched laminate (TSL) in suppressing damage along the characteristic distance.

Stress–strain behaviour

Figure 7 depicts the open-hole tension finite element and the experimental result validation on LSLs and TSLs at a characteristic length (y–a) at 1 mm. These graphs show an error of 5.18% and 4.97% at 1 mm characteristic length with experimental data for open-hole LSLs (Fig. 7*a*) and TSLs (Fig. 7*b*), respectively.

The stress distribution in Fig. 8 shows that along the x direction, each laminate has a unique stress distribution. The stress distribution has also been observed at the laminate and stitches individually, as shown in Figs. 8 and 9. To draw a conclusion for the failure, first the maximum stress point as damage initiation point for the composite and stitch was identified, and then the through thickness stress was extracted at that point. Similarly, the through thickness stress at the centre of the discontinuity was plotted as illustrated in Fig. 10. These figures indicate that the outermost layers are more susceptible to failure than the inner laminates.

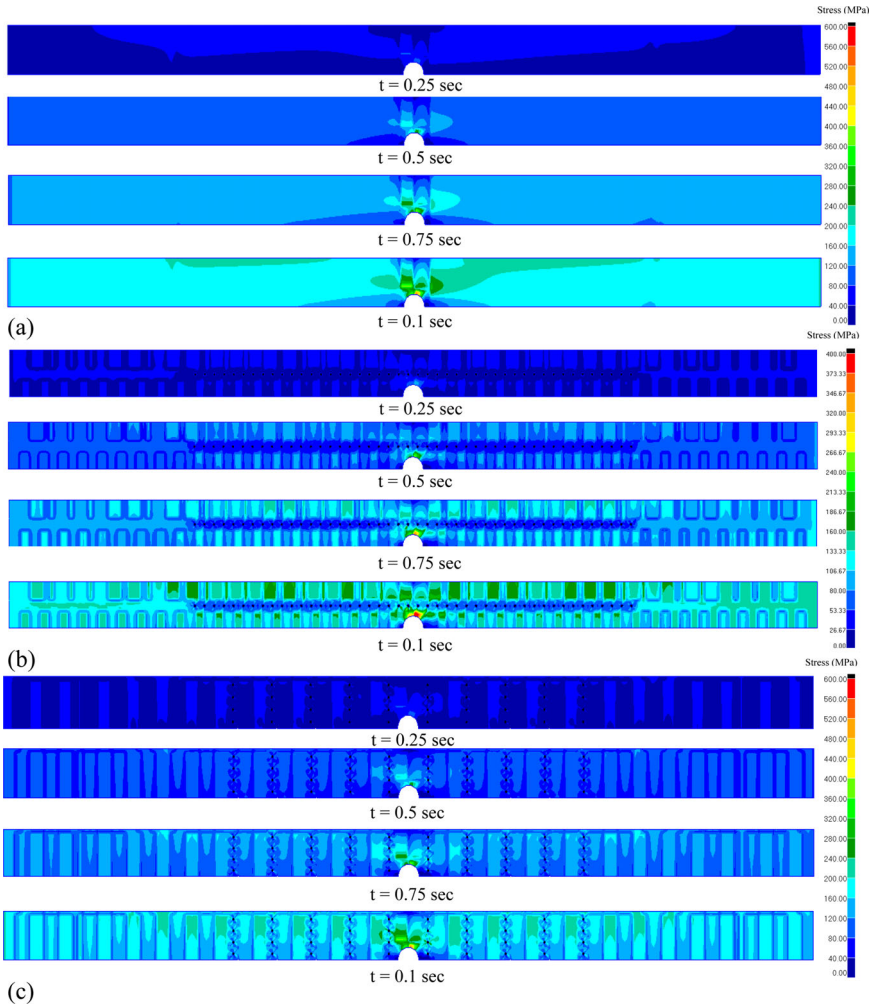

8 Stress history for open-hole laminates: *a* unstitched; *b* longitudinally stitched; *c* transversely stitched

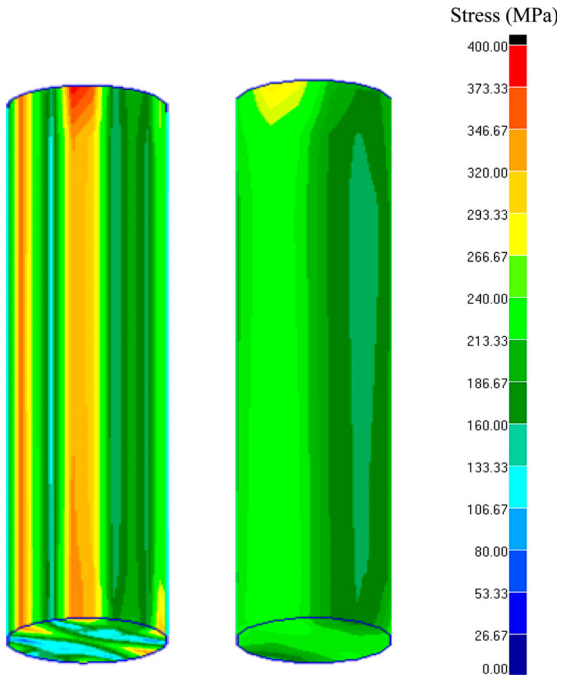

9 Through thickness stress counters: *a* longitudinal stitch; *b* transverse stitch

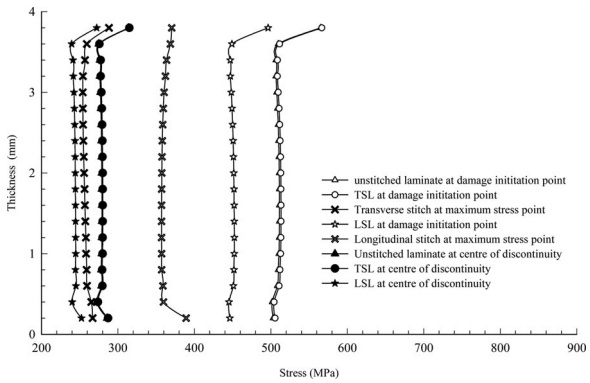

10 Through thickness stress distribution at different points for open-hole laminates

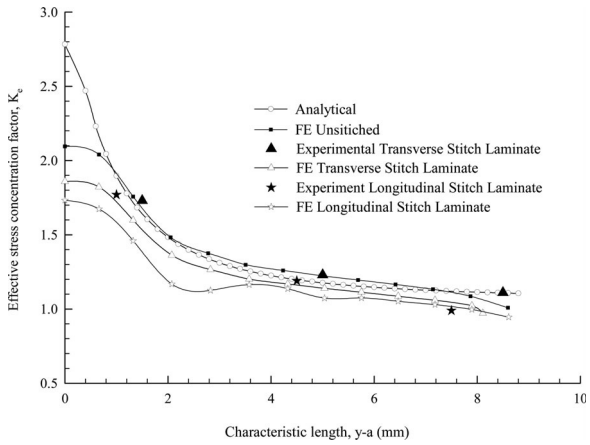

11 Stress concentration factor distribution for laminates

SCF visualisation

Figure 11 shows the effective SCF for the analytical solution and FEA solution for unstitched and stitched laminates. These graphs illustrate that a transversely stitched open-hole laminate has a reduced effective SCF by 8.07% compared to unstitched laminates. Similarly, the effective SCF of the longitudinally stitched open-hole laminate is reduced by 14.29 and 21.22% compared to the transversely stitched and unstitched open-hole laminates, respectively. Note that these comparisons have been conducted with the corresponding node at the characteristic length. Thus, unstitched laminates had a higher notch sensitivity than TSLs, and the TSLs had a higher notch sensitivity than the LSLs. This result arises because the crack is propagated towards the characteristic length and because a longitudinal stitch is able to suppress damage propagation effectively due to its orientation.

Conclusion

An accurate and efficient numerical analysis of open-hole laminates reinforced with stitches along different orientation at the macroscopic structural level has been validated by experimental results. This kind of detailed analysis is expected to be helpful for designers seeking to understand stitched laminate fracture behaviour in depth. Based on the numerical simulations, the following points are highlighted:

- Progressive failure analysis using Puck's failure criteria has been shown to be capable of characterising fracture propagation along with the effect of stitch orientation, which plays a vital role in suppression of damage on the discontinuous structure.
- The finite element result is consistent with experimental stress–strain results with less than a 5% error. Furthermore, this method is capable of predicting SCF behaviour with a good correlation with analytical

results, which was not otherwise clear before performing the experiment.
- SCF was reduced through stitching by 21 and 8% for longitudinal and transverse stitches along the notch respectively, compared to unstitched open-hole laminates. The reduced SCF corresponds to an improvement in structural performance.
- Longitudinally stitched open-hole laminates are more effective than TSLs under applied uniaxial tension loading. Longitudinal stitching decreases notch sensitivity and improve notch strength more than transverse stitching, and TSLs are similarly superior to unstitched open-hole laminates.

Acknowledgements

Authors would like to thank Tokyo Metropolitan Government for the financial support from Asian Network of Major Cities 21 (ANMC-21) project. Author would like to thank Dr Arief Yudhanto from KAUST for valuable suggestions.

References

1. O. O. Ochoa and J. N. Reddy: 'Finite element analysis of composite laminates', 1992, Dordrecht, The Netherlands, Kluwer Academic Publishers.
2. M. C.-Y. Niu: 'Composite airframe structures: practical design information and data', 1992, Los Angeles, USA, Techincal Book Co.
3. K. A. Dransfield, L. K. Jain and Y.-W. Mai: 'Improving the delamination resistance of CFRP by stitching-a review', *Compos. Sci. Technol.*, 1994, **50**, 305–317.
4. K. A. Dransfield, L. K. Jain and Y. W. Mai: 'On the effects of stitching in CFRPs-I. mode I delamination toughness', *Compos. Sci. Technol.*, 1998, **58**, 815–827.
5. L. K. Jain, K. A. Dransfield and Y.-W. Mai: 'On the effects of stitching in CFRP-II. mode II delamination toughness', *Compos. Sci. Technol.*, 1998, **58**, 829–837.
6. A. P. Mouritz and B. N. Cox: 'A mechanistic interpretation of the comparative in-plane mechanical properties of 3D woven, stitched and pinned composites', *Compos. A: Appl. Sci. Manuf.*, 2010, **41**, 709–728.
7. A. P. Mouritz, J. Gallagher and A. A. Goodwin: 'Flexural and interlaminar shear properties of stitched GFRP laminates following repeated impacts', *Compos. Sci. Technol.*, 1997, **57**, 509–522.
8. A. P. Mouritz, K. H. Leong and I. Herszberg: 'A review of the effect of stitching on the in-plane mechanical properties of fibre-reinforced polymer composites', *Compos. A: Appl. Sci. Manuf.*, 1997, **28A**, 979–991.
9. L. C. Dickinson: 'A designed experiment in stitched/RTM composites', 1995, Virginia, USA, Langley Research Centre, NASA.
10. H. J. Chun, H. W. Kim and J. H. Byun: 'Effect of through-the-thickness stitches on elastic behavior of multi-axial warp knit fabric composites', *Compos. Struct.*, 2006, **74**, 484–494.
11. L. Chen, P. G. Ifju and B. V. Sankar: 'Analysis of mode I and mode II tests for composites with translaminar reinforcements', *J. Compos. Mater.*, 2005, **39**, 1311–1333.
12. L. Tong, A. P. Mouritz and M. K. Bannister: '3D fibre reinforced polymer composites', 2002, Oxford, UK, Elsevier Science Ltd.
13. J. Herwan, A. Kondo, S. Morooka and N. Watanabe: 'Effect of stitch density and stitch thread thickness on mode II delamination properties of vectran stitched composites', *Plast. Rubber Compos.*, 2014, **43**, 300–308.
14. D. T. Fishpool, A. Rezai, D. Baker, S. L. Ogin and P. A. Smith: 'Interlaminar toughness characterisation of 3D woven carbon fibre composites', *Plast. Rubber Compos.*, 2013, **42**, 108–114.
15. S. D. Green, M. Y. Matveev, A. C. Long, D. Ivanov and S. R. Hallett: 'Mechanical modelling of 3D woven composites considering realistic unit cell geometry', *Compos. Struct.*, 2014, **118**, 284–293.
16. T. Ishikawa and T.-W. Chou: 'Stiffness and strength behaviour of woven fabric composites', *J. Mater. Sci.*, 1982, **17**, 3211–3220.
17. T.-W. Chou and T. Ishikawa: 'One-dimensional micromechanical analysis of woven fabric composites', *AIAA J.*, 1983, **21**, 1714–1721.
18. N. K. Naik and R. Kuchibhotla: 'Analytical study of strength and failure behaviour of plain weave fabric composites made of twisted yarns', *Compos. A: Appl. Sci. Manuf.*, 2002, **33**, 697–708.
19. B. N. Cox, W. C. Carter and N. A. Fleck: 'A binary model of textile composites-I. formulation', *Acta Metall. Mater.*, 1994, **42**, 3463–3479.
20. J. Xu, B. N. Cox, M. A. McGlockton and W. C. Carter: 'A binary model of textile composites-II. The elastic regime', *Acta Metall. Mater.*, 1995, **43**, 3511–3524.
21. M. A. McGlockton, B. N. Cox and R. M. McMeeking: 'A binary model of textile composites:III high failure strain and work of fracture in 3D weaves', *J. Mech. Phys. Solids*, 2003, **51**, 1573–1600.
22. P. P. Camanho, C. G. Dávila, S. T. Pinho and J. J. C. Remmers: 'Mechanical response of composites: computational methods in applied ciences', 2008. Barcelona, Spain, International Center for Numerical Methods in Engineering (CIMNE).
23. M. H. Dirikolu and A. Aktas: 'Analytical and finite element comparisons of stress intensity factors of composite materials', *Compos. Struct.*, 2000, **50**, 99–102.
24. Z. Yun, C. Xiaoquan and Y. Baig: 'Effect of stitching on plain and open-hole strength of CFRP laminates', *Chin. J. Aeronaut.*, 2012, **25**, 473–484.
25. M. R. Wisnom and S. R. Hallett: 'The role of delamination in strength, failure mechanism and hole size effect in open hole tensile tests on quasi-isotropic laminates', *Compos. A: Appl. Sci. Manuf.*, 2009, **40**, 335–342.
26. B. G. Green, M. R. Wisnom and S. R. Hallett: 'An experimental investigation into the tensile strength scaling of notched composites', *Compos. A: Appl. Sci. Manuf.*, 2007, **38**, 867–878.
27. S. R. Hallett, B. G. Green, W. G. Jiang and M. R. Wisnom: 'An experimental and numerical investigation into the damage mechanisms in notched composites', *Compos. A: Appl. Sci. Manuf.*, 2009, **40**, 613–624.
28. R. M. O'Higgins, M. A. McCarthy and C. T. McCarthy: 'Comparison of open hole tension characteristics of high strength glass and carbon fibre-reinforced composite materials', *Compos. Sci. Technol.*, 2008, **68**, 2770–2778.
29. H. Thuis and E. Bron: 'The effect of stitching density and laminate lay-up on the mechanical properties on stitched carbon fabrics', 1996, Marknesse, Netherlands, National Aerospace Laboratory NLR.
30. M. Z. S. Khan and A. P. Mouritz: 'Fatigue behaviour of stitched GRP laminate', *Compos. Sci. Technol.*, 1996, **56**, 695–701.
31. Z. Junqian and W. Yuqing: 'A predictive approach to the in-plane mechanical properties of stitched composite laminates', *Acta Mech. Solida Sinica*, 2007, **20**, 130–140.
32. X. P. Han, L. X. Li, X. P. Zhu and Z. F. Yue: 'Experimental study on the stitching reinforcement of composite laminates with a circular hole', *Compos. Sci. Technol.*, 2008, **68**, 1649–1653.
33. K. Gliesche, T. Hubner and H. Orawetz: 'Application of the tailored fibre placement(TFP) process for a local reinforcement on an "open-hole" tension plate from carbon/epoxy laminates', *Compos. Sci. Technol.*, 2003, **63**, 81–88.
34. A. Yudhanto, N. Watanabe, Y. Iwahori and H. Hoshi: 'The effect of stitch orientation on the tensile and open hole tension properties of carbon/epoxy plain weave laminates', *Mater. Des.*, 2012, **35**, 563–571.
35. P. Joshi, A. Kondo and N. Watanabe: 'Numerical analysis of carbon fibre/epoxy stitched laminates with varied through thickness stitched density', European Conference on Composite Materials-17, 2016.
36. M. A. Portanova and J. E. Masters: 'Standard methods for open hole tension testing of textile composites', 1995, Virginia, USA, Langley Research Centre, NASA.
37. P. Joshi, S. Morooka, A. Kondo, H. Hoshi and N. Watanabe: 'Numerical analysis of carbon-fibre/epoxy reinforced composite laminates with varied stitched density on tensile loading', Korea–Japan Joint Symposium on Composite Materials-10, 2016.
38. P. Tan, L. Tong and G. P. Steven: 'A three-dimensional modelling technique for predicting the linear elastic property of opened-packing woven fabric unit cells', *Compos. Struct.*, 1997, **38**, 261–271.
39. Y. Yasui, F. Hori, M. Amano and J. Takeuchi: 'Method and apparatus for production of a three-dimensional fabric', US Patent., 1998, **5**, 772, 821, 21.
40. S. K. Parida and A. K. Pradhan: '3D finite element analysis of stress distributions and strain energy release rates of adhesive bonded flat composite lap shear joints having preexisting delaminations', *J. Mech. Sci. Technol.*, 2014, **28**, 481–488.

41. P. T. Cheuk and L. Tong: 'Failure of adhesive bonded composite lap shear joints with embedded precrack', *Compos. Sci. Technol.*, 2002, **62**, 1079–1095.
42. K.-J. Bathe: 'Finite element procedures', 1996, New Jersey, Prentice Hall Ltd.
43. M. Knops: 'Analysis of failure in fiber polymer laminates: the theory of alfred Puck', 2008, Leipzig, Germany, Springer.
44. M. J. Hinton and A. S. Kaddour: 'Benchmarking of triaxial failure criteria for composite laminates: Comarision between models of "Part(A) of "WWFE-II"', *J. Compos. Mater.*, 2012, **46**, 2595–2634.
45. A. Kaddour and M. Hinton: 'Maturity of 3D failure criteria for fibre-reinforced composites: Comparison between theories and experiments: Part B of WWFE-II', *J. Compos. Mater.*, 2013, **47**, 925–966.
46. M. J. Hinton, A. S. Kaddour and P. D. Soden: 'Failure criteria in fibre reinforced polymer composites', 2004, Oxford, UK, Elsevier Science Ltd.
47. E. J. Barbero: 'Introduction to composite material design', 1999, New York, USA, Taylor & Francis Group.
48. A. Ataş: 'Open hole compressive strength and damage mechanism: maximum stress versus Hasin criteria', *Plast. Rubber Compos.*, 2015, **44**, 280–290.
49. Y. Tanzawa, N. Watanabe and T. Ishikawa: 'FEM simulation of modified DCB test for 3-D orthogonal interlocked fabric composites', *Compos. Sci. Technol.*, 2001, **61**, 1097–1107.